**Full Paper:** The functionalization of polystyrene/poly(ethylene glycol) TentaGel® microbeads ($d = 20$ μm) with 2,2′:6′,2″-terpyridine units is described resulting in a material with easily accessible ligands which possess an excellent affinity for transition metal ions. The subsequent loading with different metal ions via metal-to-ligand complexation yielded the corresponding $Co^{II}$, $Ni^{II}$, $Fe^{II}$, and $Cu^{II}$ modified beads. The isolated materials were investigated in detail utilizing UV/vis spectroscopy, optical microscopy, atomic absorption spectroscopy (AAS), scanning electron microscopy (SEM), and atomic force microscopy (AFM). Moreover, grafting of free terpyridine moieties via ruthenium(II)/ruthenium(III)-chemistry onto the beads is demonstrated. This opens-up new pathways for the selective modification of such microbeads and the preparation of functional materials.

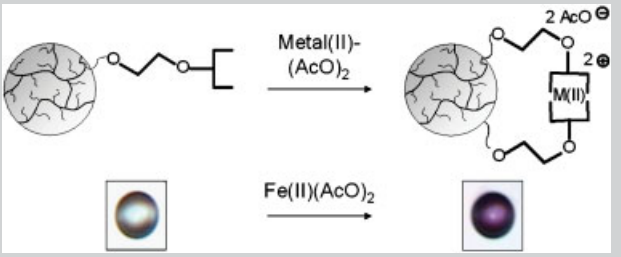


Scheme of the formation of bis-terpyridine-metal complexes bound to polystyrene/poly(ethylene glycol) TentaGel® microbeads.

# Terpyridine-Functionalized TentaGel Microbeads: Synthesis, Metal Chelation and First Sequential Complexation[a]

*Ulrich S. Schubert,**[1,2] *Alexander Alexeev,*[1] *Philip R. Andres*[1,2]

[1] Laboratory of Macromolecular Chemistry and Nanoscience, Eindhoven University of Technology and Dutch Polymer Institute, P. O. Box 513, 5600 MB Eindhoven, The Netherlands
Fax: 0031 40 247 4186; E-mail: u.s.schubert@tue.nl
[2] Center for Nanomaterials (CeNS), LMU München, Geschwister-Scholl-Platz 1, 80333 München, Germany

Received: May 25, 2003; Revised: August 21, 2003; Accepted: September 3, 2003; DOI: 10.1002/mame.200300140

**Keywords:** chelating resin; microbeads; supramolecular structures; terpyridine; transition metal chemistry

## Introduction

The coupling of ligands capable of complexing transition metal ions or the immobilization of the corresponding organometallic species on support materials has been of great interest for decades.[1] Besides utilization in the development of new catalysts with specific activities, the simple isolation and recycling properties of such functionalized support materials are of importance. Therefore, such beads also play an important role in combinatorial chemistry.[2] Moreover, the selective uptake of certain transition metal ions is attractive for environmental purposes.[3] Finally, new functional materials can be envisioned by the combination of metal complexes with special electrochemical and photochemical properties and solid support materials. One well-known problem for such heterogeneous systems is leaching of the metal ions, e.g., in the case of phosphines as ligands.[4] Therefore, recent approaches include the use of poly(pyridine)s as chelating ligands. 2,2′-Bipyridine and 2,2′:6′,2″-terpyridine units present two of the most prominent types of *N*-heterocyclic ligands for transition metal ions and are widely used in analytical and supramolecular chemistry as well as material science.[5] In particular, terpyridine ligand systems offer a wide range of specific properties, such as complexation of a variety of interesting transition metal ions (such as cobalt, nickel, ruthenium, copper, manganese, zinc, etc.), leading to very high stability constants, and interesting physical properties of the corresponding metal complexes.[5] Besides the free ligand

[a] Supporting information for this article is available on the journal's homepage at http://www.mme-journal.de or from the author.

 

systems or closely related substituted or functionalized compounds, the incorporation of terpyridine ligands into linear copolymers was described recently.[6] However, the immobilization of the terpyridine ligands onto solid supports would open additional opportunities for applications, such as in catalysis, metal chelation from contaminated solutions, combinatorial chemistry, functional materials, or the selective grafting of compounds or nano-objects. In particular, the combination with polymer-based beads is of interest. Surprisingly little has been done so far in this direction. Most of the examples described use low-molar-mass derivatives or ligands bound to linear, soluble polymers. In the case of bipyridine, several examples are also described where the ligand is bound to a solid substrate.[7] In particular, polystyrene beads are utilized for this immobilization. However, the recent strongly growing interest in the utilization of terpyridine ligands and its corresponding metal complexes is at present not really displayed regarding the heterogenization. Only very few papers describe the immobilization onto planar substrates (e.g., via layer-by-layer self-assembly processes[8]) or beads. Of the latter case, to the best of our knowledge, only three examples exist: The copolymerization of norbornene-terpyridine derivatives and subsequent immobilization on silica particles[9] and the functionalization of polystyrene beads with terpyridine ligands.[10,11] Yoo et al.[11] used a direct reaction of the styrene moieties and the corresponding terpyridine derivative. Therefore the authors claim to have established a very rigid connection, which did not allow the formation of the typical octahedral bis-complexes upon addition of transition metal salts. These two known examples both use a rather rigid connection to the polystyrene bead material, where the functionalized chloromethylstyrene or silyl-chloride-styrene units are reacted with the phenyl-terpyridine or terpyridine in the 4′-positions. Such a stiff connection should prevent the formation of octahedral bis-complexes to a great extent. Therefore, uncommon and usually not stable mono-complexes can be isolated and utilized for catalytic purposes, such as the iron(III) mono(terpyridine) complex.[11] In order to allow a high loading rate with transition metal ions through the formation of bis-complexes, a different connection approach was selected, starting from hydroxyl-functionalized TentaGel microbeads.[12,13] TentaGel microbeads consist of a cross-linked polystyrene core with grafted-on hydroxy-terminated poly(ethylene glycol) side chains and combine the advantages of gelatinous resins (such as the well-known 1% cross-linked polystyrene resins or cross-linked poly(acrylamide)s) and macro-porous resins (Kieselgur, glass or highly cross-linked polystyrene). This hybrid-type resin, therefore, to some extent allows solid-phase chemistry under liquid-phase conditions. The 4′-chloro-2,2′:6′,2″-terpyridine[14,15] was chosen as functionalized terpyridine unit which can be easily synthesized in multi-gram quantities and is also commercially available.

Here we report a new immobilization route for terpyridine ligands onto poly(ethylene glycol)-grafted polystyrene beads resulting in flexible and highly accessible metal complexing resins. Moreover, the loading with different metal ions, as well as initial grafting experiments, are described in detail.

## Experimental Part

### *Materials*

Hydroxy-functionalized TentaGel microbeads **1** ($d = 20$ μm, capacity: 0.23 $\text{mmol} \cdot \text{g}^{-1}$) were purchased from Rapp-Polymere. 2,2′:6′,2″-Terpyridine (98%), cobalt(II) acetate tetrahydrate (99.999%), nickel(II) acetate tetrahydrate (99.998%), copper(II) acetate monohydrate (99.99+%), iron(II) acetate (99.995%), and ruthenium(III) chloride were purchased from Aldrich. KOH (85%) was obtained from Merck. Chloroform and methanol were purchased from Biosolve Ltd. (both AR quality). Dimethyl sufoxide (DMSO) (99.7%) was obtained from Acros and dried over molecular sieves (3 Å) before use. 4′-Chloro-2,2′:6′,2″-terpyridine was synthesized as described elsewhere.[15]

### *Instruments*

UV/vis spectra were recorded on a Perkin-Elmer Lambda 45 UV/VIS spectrometer. Atomic force microscopy (AFM) measurements and optical microscopy were performed on a NT-MDT Solver P7LS (with integrated optical microscope). Scanning electron microscopy (SEM) images were obtained using a Jeol 840a. FT-IR spectra were recorded on a Perkin-Elmer Spectrum One. Atomic absorption spectroscopy (AAS) measurements were performed on a Shimadzu AA 6200.

### *Functionalization of the TentaGel Resin*

The resin **1** (499 mg, 0.10–0.15 mmol hydroxy functionality) was suspended in DMSO (50 mL), an excess of KOH (84 mg, 1.5 mmol) was added and the mixture was stirred at 60 °C. After 20 min, 4′-chloro-2,2′:6′,2″-terpyridine **2** (203 mg, 0.768 mmol) was added and stirring was continued for 48 h at 60 °C. The reaction mixture was poured into water (450 mL) and the microbeads were filtered off. The product was washed with deionized water (5 × 40 mL), chloroform (5 × 40 mL), and dried under vacuum to yield **3** as a yellow solid material.

UV/vis (suspension $CHCl_3$/MeOH as 1:1): $\lambda_{max}/\text{nm} = 277$.

FT-IR: 1 583, 1 564, 798 $\text{cm}^{-1}$.

**1**: Calcd. (+4 wt.-% $H_2O$) C 63.1, H 8.8, N 0.0; Found: C 63.1, H 8.8, N 0.0.

**2**: Calcd. (+4 wt.-% $H_2O$) C 64.0, H 8.6, N 1.1; Found: C 64.5, H 8.6, N 1.1.

In order to prove the successful removal of free terpyridine, small amounts of the filtrate were treated with iron(II) chloride, whereby no formation of colored iron(II) terpyridine complexes could be observed.

The bead functionalization reaction described above was also performed in the absence of the base KOH. In

 

this case, the nucleophilic aromatic substitution reaction cannot work. However, any inclusion or adsorption of the terpyridine moieties inside the TentaGel microbeads should still take place. After the work-up, no terpyridine signals in UV/vis spectroscopy or FT-IR spectroscopy could be detected. Moreover, no coloring of the bead material upon addition of iron(II) chloride was observed, proving that, indeed, no inclusion or adsorption of terpyridines took place.

### *General Preparation of the Loading with Metal Ions*

The terpyridine-functionalized beads **3** (50.0 mg) were suspended in $CHCl_3$/MeOH (2.5 mL/2.5 mL) and an excess of metal salt was added as follows: **4a**: $Fe(OAc)_2$ (3.7 mg, 0.021 mmol), **4b**: $Cu(OAc)_2 \times H_2O$ (4.0 mg, 0.020 mmol), **4c**: $Co(OAc)_2 \times 4\ H_2O$ (5.0, 0.024 mmol). **4d**: $Ni(OAc)_2$ (6.2 mg, 0.025 mmol), and **5**: $RuCl_3$ (8.1 mg, 0.033 mmol). The loading was carried out by mixing, with the help of an ultrasonic bath, for 1 h at room temperature. The beads were then filtered off and washed carefully (no vacuum) with $CHCl_3$/MeOH (1:1, $4 \times 5$ mL) and dried under vacuum to yield the differently colored microbeads.

**4a:** FT-IR: 1 615 $cm^{-1}$; UV/vis (suspension $CHCl_3$/MeOH, 1:1): $\lambda_{max}/nm = 559$ (MLCT), 319 ($\pi^* \leftarrow \pi$). **4b:** FT-IR: 1 616, 1 573 $cm^{-1}$. **4c**: FT-IR: 1 615 $cm^{-1}$. **4d**: FT-IR: 1 614, 1 573 $cm^{-1}$. **5**: FT-IR: 1 613, 1 556 $cm^{-1}$.

### *General Preparation of the Grafting Experiments*

The terpyridine-$Ru^{III}$ functionalized beads **5** (10.0 mg, capacity 0.002–0.003 mmol $Ru^{III}$-terpyridine) were suspended in ethanol (10 mL). Subsequently, a drop of *N*-ethyl morpholine and a 10-fold excess of the terpyridine ligand (0.025 mmol) was added and the mixture gently stirred under reflux for 24 h. The beads were then filtered off and washed with ethanol, methanol, and dichloromethane (each $3 \times 30$ mL). The terpyridine complex grafted beads **6** and **7** were isolated as a red material.

**6**: FT-IR: 1 615, 1 545 $cm^{-1}$; UV/vis (suspension $CHCl_3$/MeOH, 1:1): $\lambda_{max}/nm = 483$ (MLCT), 305 ($\pi^* \leftarrow \pi$, terpyridine).

**7**: FT-IR: 1 716, 1 662, 1 610, 1 543 $cm^{-1}$; UV/vis (suspension $CHCl_3$/MeOH, 1:1): $\lambda_{max}/nm = 498$ (MLCT), 386, 367, 347 ($\pi^* \leftarrow \pi$, anthracene), 310 ($\pi^* \leftarrow \pi$, terpyridine).

### *AAS Measurements*

General procedure for sample preparation (**4a**, **4b**, and **4c**): Between 6 and 8 mg of the loaded beads (as well as the HO-beads for the test experiments) were oxidized in 1 mL $H_2SO_4$ and 0.5 mL $H_2O_2$. After complete oxidation, the solution was diluted with deionized water to an expected metal concentration of exactly 2.5 ppm. For the preparation of the calibration curves, a solution containing the same concentration of $H_2SO_4/H_2O_2$ was utilized. The calibration curves (five calibration points, 1 to 5 ppm) of all measurements as well as the test measurements revealed an $R^2$ value of $\geq 0.996$.

## Results and Discussion

### *Functionalization of TentaGel Beads with 2,2′:6′,2″-Terpyridine*

In order to obtain a high functionalization degree of the resin with the *N*-heterocyclic ligand, the hydroxy-functionalized TentaGel microbeads **1** were reacted with an excess of 4′-chloro-2,2′:6′,2″-terpyridine **2** in DMSO in the presence of KOH (Scheme 1). The reaction conditions were optimized earlier for the reaction of **1** with small hydroxy-terminated organic entities[16] as well as linear poly(ethylene glycol)s.[6] The resulting oxo-ether bridged 2,2′:6′,2″-terpyridine functionalized resin **3** was thoroughly washed several times with a mixture of $CHCl_3$/MeOH (1:1) to remove the excess of unreacted 4′-chloro-2,2′:6′,2″-terpyridine. Subsequently, the terpyridine-functionalized beads were characterized by standard techniques. The UV/vis spectrum revealed a strong intense band around 280 nm, which can be assigned to the $\pi^* \leftarrow \pi$ bands of the terpyridine ligand. The IR spectrum showed the typical pyridine valence vibrations around 1 570 and 800 $cm^{-1}$ (Figure 1, the OH-band is visible in both cases because of the large water-uptake of the TentaGel beads). Moreover, addition of iron(II) chloride to the beads immediately resulted in an intense purple coloring of the beads, typical for the bis-terpyridine-iron(II) complexes. In order to avoid any misinterpretation by eventually non-covalently included terpyridine ligands, a test reaction was performed (see experimental part). From the elemental analysis, it also becomes obvious that functionalization has taken place. The measured values, especially for nitrogen, match the calculated values for quantitative terpyridine functionalization. However, it has to be taken into account that the calculated values are based on the bead manufacturers maximum poly(ethylene glycol) weight percentage of 70% poly(ethylene glycol) for HO-bead **1**. Taking this value as basis for the calculation of the elemental analysis of the commercially obtained HO-bead **1**, the measured elemental analysis only leads to a match with the calculated one if a water content of 4 weight percent is taken into account. Nevertheless, even taking other percentages of PEO/PS, slightly different water contamination, and errors of measurement into account, a degree of functionalization larger than 95% can be concluded.

### *Metal Ion Loading of the Terpyridine Beads*

The prepared terpyridine-functionalized microbeads should be suitable for the complexation of a wide range of transition metal ions in a solution-like behavior, whereby the poly(ethylene glycol) spacers would enable a high flexibility of the metal complexing unit. To investigate the complexation properties, the microbeads were treated with several metal salts. For this purpose, beads were suspended in $CHCl_3$/MeOH (1:1) and an excess of the corresponding

 

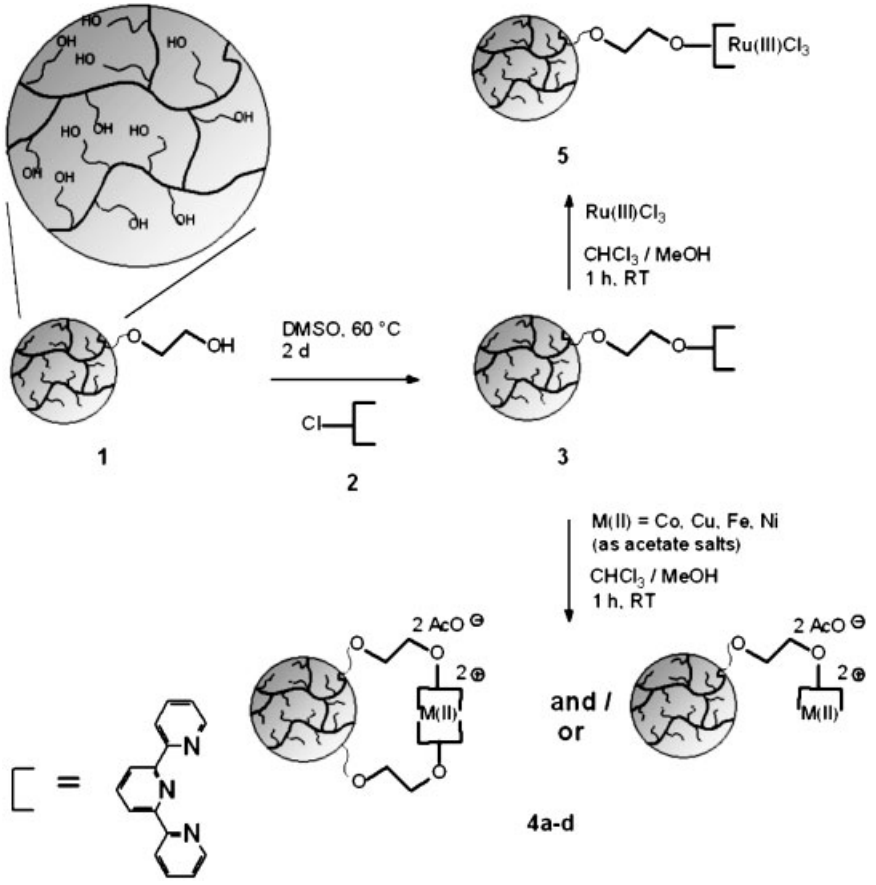


Scheme 1. Schematic representation of the functionalization of the hydroxy-functionalized microbeads **1** with 4′-chloro-2,2′:6′,2″-terpyridine **2** and the subsequent loading with different metal salts.

metal salt ($Fe(OAc)_2$, $Co(OAc)_2$, $Cu(OAc)_2$, and $Ni(OAc)_2$) was added. After mixing with the help of an ultrasonic bath for 1 h in order to ensure complete swelling and mixing[12,13] (the reactions of these metal ions with terpyridine in non-heterogeneous systems is immediate[5a]), the beads were filtered off, washed, and dried. Depending on the metal salt utilized, the corresponding typical color of the corresponding terpyridine metal complex was observed (Figure 2). This optical observation could be further confirmed by UV/vis spectroscopy. As an example, the comparison of the iron-loaded bead **4a** with the hydroxy (**1**) and terpyridine-functionalized (**3**) beads are shown in Figure 3 (the spectra were recorded in a suspension which was prepared by mixing in an ultrasonic bath, see also ref.[17] for a similar procedure). The red shift of the $\pi^* \leftarrow \pi$ band, and the appearance of the metal-to-ligand-charge-transfer (MLCT) band at 559 nm, clearly indicated the successful formation of the terpyridine-iron(II) bis-complex. This example demonstrates the high flexibility and accessibility of the terpyridine ligands attached to the microbead via poly(ethylene glycol) spacer units in contrast to the recently described direct coupling of the terpyridine units to the polystyrene moieties. In order to further investigate the loading capabilities of the terpyridine-functionalized beads, the metal contents of the beads after the loading reactions were determined by atomic absorption spectrometry (AAS)

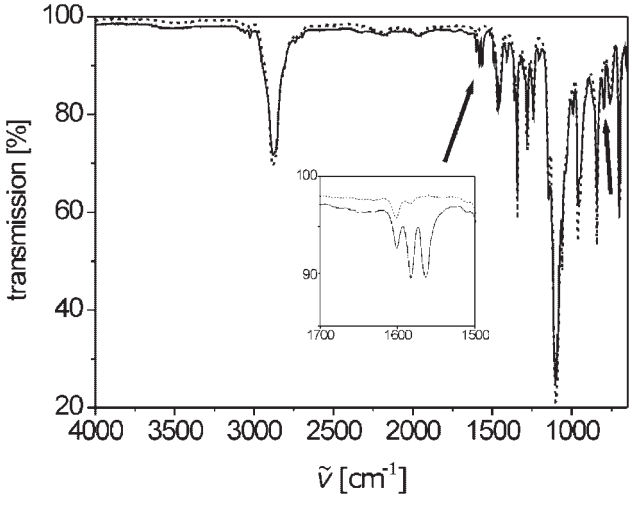


Figure 1. Comparison of the FT-IR spectra of the hydroxy-functionalized microbeads **1** (starting material, - - -) and the 2,2′:6′,2″-terpyridine-functionalized microbeads **3** (—).

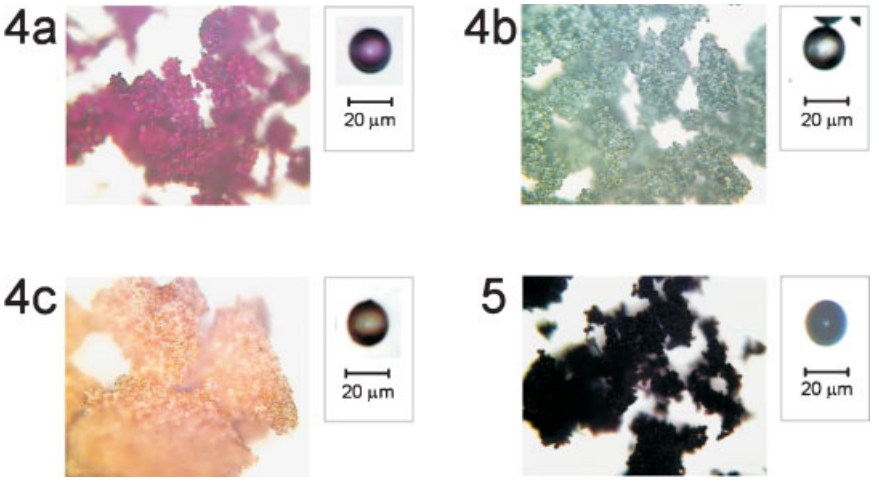


Figure 2. Pictures of the different metal ion-loaded beads: **4a**: $Fe^{II}$, **4b**: $Cu^{II}$, **4c**: $Co^{II}$, **5**: $Ru^{III}$ (calibrated sizes).

for the cases of loading with iron(II), cobalt(II), and copper(II) acetates. In order to prepare measurable aqueous solutions of the beads, a destructive method was applied for sample preparation. The loaded beads were oxidized in a mixture of sulfuric acid and peroxide. Subsequently, an aqueous solution leading to a suitable metal concentration for the AAS measurements was prepared. Additionally, in order to exclude unspecific binding of metal acetate to the bead material, test loadings with the HO-bead and preparation of AAS samples were done in the same way. These test measurements proved that no unspecific binding of metal acetate to the bead took place (Table 1). Furthermore, it is apparent that copper acetate seems to form preferably mono-complexes as opposed to the cobalt and iron acetates, which is also known for non-heterogeneous systems.[5a,18]

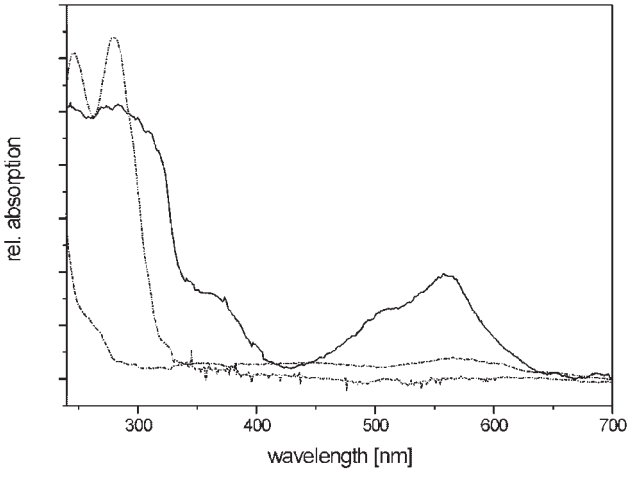


Figure 3. UV/vis spectra of $Fe^{II}$-loaded terpyridine beads **4a** (—), terpyridine beads **3** (· · ·), and HO-beads **1** (· – ·) all measured in $CHCl_3$/MeOH (1:1, suspension, approx. 0.5 mg · $L^{-1}$).

These first loading results also indicate that such beads can selectively form mono or bis-complexes, depending on the metal salt utilized.

### *Characterization with SEM and AFM*

The prepared terpyridine-functionalized as well as metal-loaded microbeads were also investigated regarding their microscopic and nanoscopic morphology. For this purpose, scanning electron microscopy (SEM) and atomic force microscopy (AFM) measurements were performed. Figure 4 shows representative SEM images of some of the functionalized beads. Comparing the hydroxy-functionalized TentaGel microbeads **1** (Figure 4a) with the terpyridine-functionalized microbeads **3** (Figure 4b) and the $Co(OAc)_2$-loaded terpyridine microbeads **4c** (Figure 4c), a trend to a smoother surface can be observed. Moreover, the hydroxy-functionalized beads revealed a stronger adhesion to each other. The fact that metal-containing beads showed a much smoother surface compared to the more wrinkled one of a ligand-functionalized bead has already been reported for a similar system.[19] It must be taken into account, though, that the observed differences could also result from the sputtering of the beads with gold, which is required for conductivity. Nevertheless, the observed features are characteristic for all investigated beads, also regarding the fact that all the samples have been prepared according to the same procedure (spreading on glass plates from a droplet of deionized water and evaporation of the water under vacuum for 20 h). Further characterization attempts using techniques that do not require gold sputtering (such as environmental SEM) are currently ongoing. The atomic force microscopy image (phase image) for the hydroxy-functionalized microbeads **1** showed a lamellar like structure, which is well known for poly(ethylene glycol)s (Figure 5). Upon functionalization with terpyridine units,

 

Table 1. Amount of metal salt bound to the terpyridine beads determined by AAS.

| Acetate salt | Loading of terpyridine-beads | Test loading of HO-bead | Expected amount for only bis-complexation | Expected amount for only mono-complexation |
|---|---|---|---|---|
| Resulting loading of terpyridine beads[a)](cap.: 0.23 mmol · $g^{-1}$) | | | | |
| $Fe^{II}$ | 0.9 | 0.0 | 1.0 | 2.0 |
| $Co^{II}$ | 1.1 | 0.0 | 1.0 | 2.0 |
| $Cu^{II}$ | 2.0 | 0.0 | 1.0 | 2.1 |
| Resulting loading of terpyridine beads[b)] | | | | |
| $Fe^{II}$ | 5.2 | 0.0 | 5.8 | 11.5 |
| $Co^{II}$ | 6.4 | 0.0 | 5.8 | 11.5 |
| $Cu^{II}$ | 11.0 | 0.0 | 5.8 | 11.5 |

[a)] In mg of acetate salt.
[b)] In $10^{-3}$ mmol.

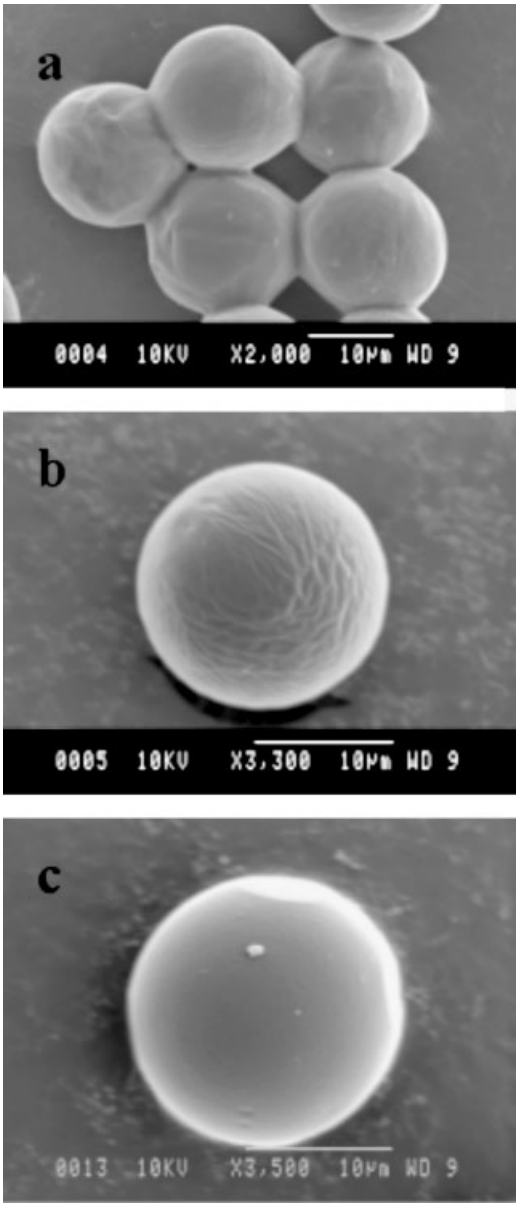


Figure 4. SEM micrographs of the commercial HO-functionalized bead **1** (a), the terpyridine-functionalized bead **3** (b), and the $Co^{II}$-loaded terpyridine bead **4c** (c).

these lamellae are not visible anymore, which could be caused by a steric disturbance induced by the rather bulky terpyridine into the poly(ethylene glycol) phase. In the case of the metal-loaded beads ($Co(OAc)_2$, **4c**), a different surface (granular structure) can be observed. At present, we are not able to present a reasonable interpretation for these findings. However, the effect might have to do with the crystallinity of the metal complex salt.

### *Sequential Functionalization Utilizing $Ru^{III}/Ru^{II}$-Terpyridine Chemistry*

Up to now, all described metal-loading experiments used unspecific complexation strategies (e.g., formation of the bis-complexes utilizing two identical ligands or mono-complexes). However, a directed coupling method utilizing ruthenium(III)/ruthenium(II) terpyridine chemistry was developed in supramolecular chemistry, which allows the selective construction of A-[Ru]-B type complexes. For this purpose, ruthenium(III) mono-terpyridine complexes represent the key intermediates. This route has been applied to isolated organic[20] as well as polymeric systems.[6] An application of this selective construction principle to beads could allow the design of a new platform for the immobilization of a wide range of compounds utilizing the terpyridine-ruthenium connection. Because of the high stability of the complexes (e.g., no exchange with competing ligands takes place over 24 h in a pH range of 0–14[21]), they can act as a stable linker for chemically modifying solid supports and therefore selectively changing the properties. This could also open new routes for developing novel heterogeneous catalytic systems. In a first experiment, the terpyridine-functionalized microbeads **3** were treated with $RuCl_3$ (Scheme 2). The resulting material **5** revealed the typical dark brown color known from terpyridine-ruthenium(III) mono complexes. Subsequently, **5** was reacted with free 2,2′:6′,2″-terpyridines as well as, in a further experiment, with free anthracene functionalized terpyridine under reducing conditions, leading to beads **6** and **7**. The reaction conditions were chosen according to known reactions utilizing ethanol as solvent as well as reducing

 

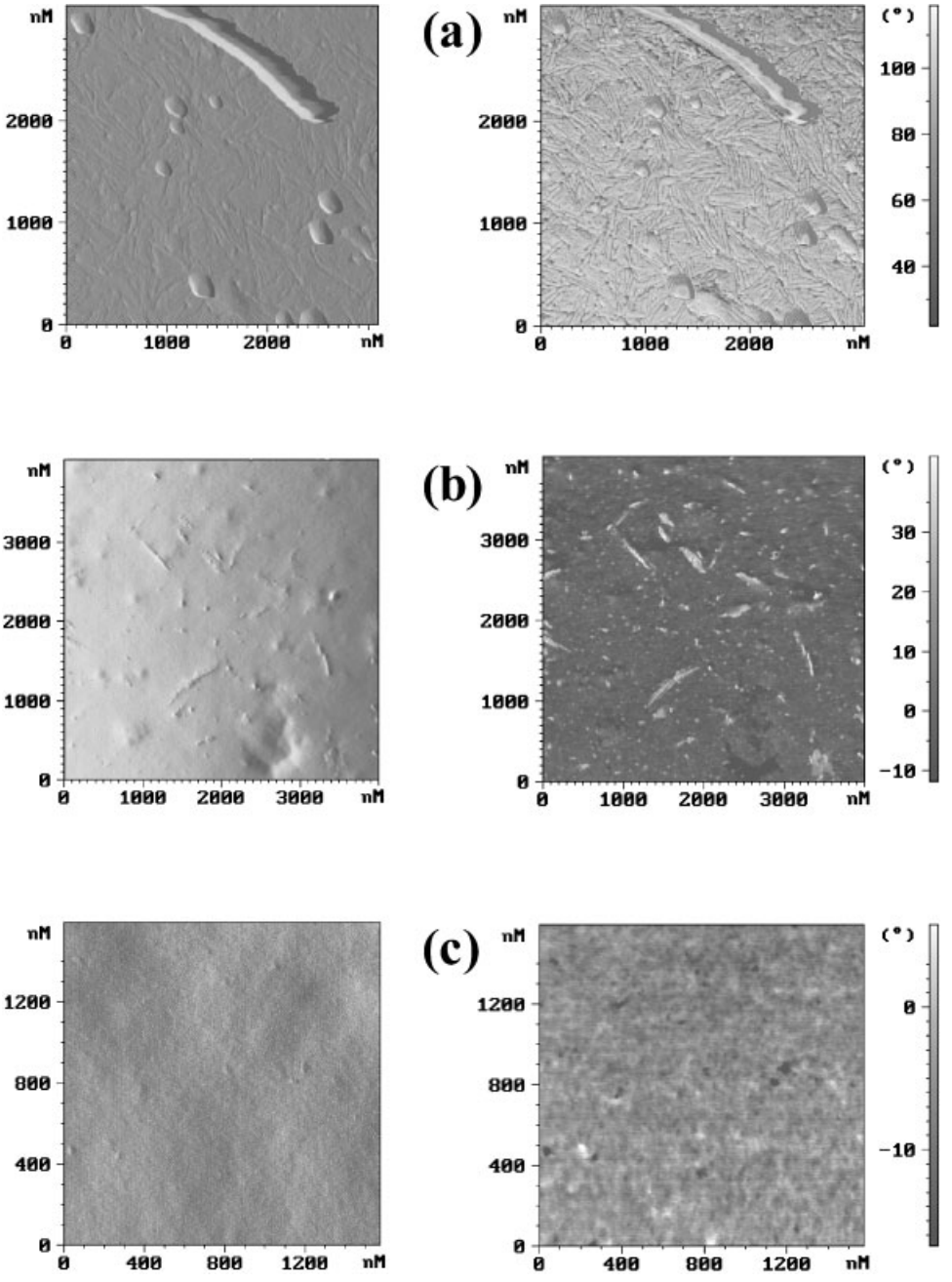


Figure 5. AFM images of the commercial OH-functionalized beads **1** (a), terpyridine-functionalized beads **3** (b), and the $Co^{II}$-loaded terpyridine beads **4c** (c). The images on the left side are height images, the images on the right represent the corresponding phase images.

agent, and *N*-ethyl-morpholine as catalyst. The success of the reaction could be clearly seen by the change in color from brown (terpyridine-ruthenium(III)) to red (bis-terpyridine-ruthenium(II)) and the macroscopic change could also be observed under the microscope (Figure 6). The UV/vis spectra of **6** (Figure 7) and **7** (Figure 8) clearly revealed the typical metal-to-ligand charge-transfer (MLCT) absorption around 490 nm (measured from suspension as described above). In addition, the anthracene functionalized material **7** showed the typical absorption

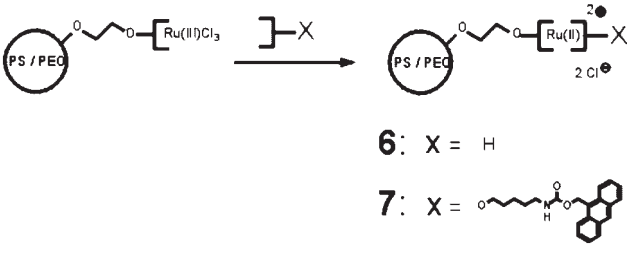


Scheme 2. Grafting-on of different functionalities via ruthenium(III)/ruthenium(II) chemistry (X = H: **6**, -R-anthracene: **7**).

 

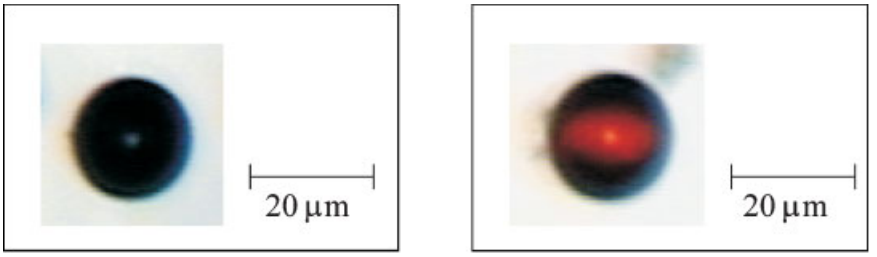


Figure 6. Microscope pictures of a $Ru^{III}$-loaded terpyridine bead **5** (left) and the terpyridine graft **6** (right).

bands for anthracene between 350 and 400 nm. Furthermore, the IR signals of the amide function of the anthracene terpyridine ligand could be observed. This data obtained from these first experiments prove that, to some extent, functionalization to unsymmetric $Ru^{II}$ bis-complexes has been successful. However, it was not possible to obtain good quantitative data for the ruthenium(III) loading or the grafting via ruthenium(II). In future, other methods, such as AAS or ICP-AES (inductively coupled plasma atomic emission spectrometry), will be used in order to address this point.

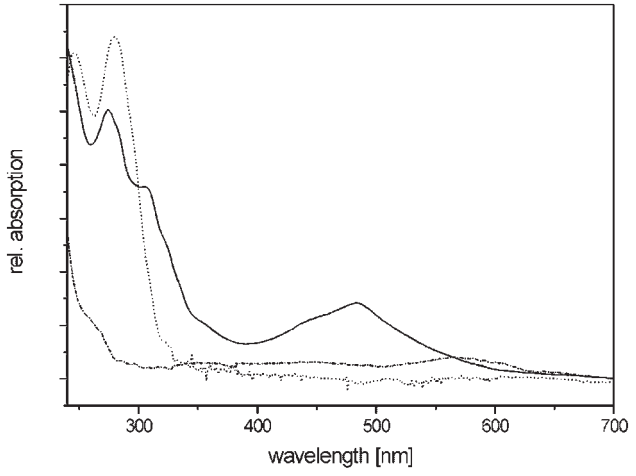


Figure 7. UV/vis spectra of terpyridine-$Ru^{II}$-grafted beads **6** (—), terpyridine beads **3** (···), and HO-beads **1** (- · -) all measured from $CHCl_3/CH_2Cl_2$ (1:1, suspension).

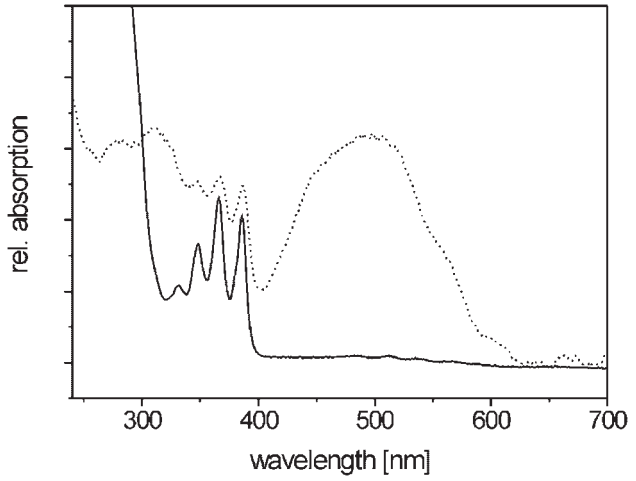


Figure 8. UV/vis spectra of anthracene-terpyridine-$Ru^{II}$-grafted beads **7** (···) and the free ligand anthracene-terpyridine (—).

## Conclusion

Metal complexing 2,2′:6′,2″-terpyridine-functionalized microbeads have been prepared by the reaction of 4′-chloro-2,2′:6′,2′-terpyridine with hydroxyl-functionalized TentaGel microbeads. The success of the reaction could be proven by UV/vis and IR spectroscopies, as well as by metal complexing tests. Moreover, the terpyridine-modified beads were complexed with several metal acetate salts ($Fe^{II}$, $Cu^{II}$, and $Co^{II}$). The loading of the beads was qualitatively characterized by UV/vis and IR spectroscopy, optical microscopy, as well as quantitatively by AAS. The AAS results illustrate that the binding of metal ion to the beads is specific; it could be shown that no unspecific complexation with the starting material, the HO-functionalized bead, takes place. In addition, surface characteristics have been investigated utilizing SEM and AFM, which indicated significant differences in surface characteristics.

Furthermore, in contrast to the described unspecific complexations on the beads, first results for the specific and directed coupling of free terpyridine ligands to the beads utilizing ruthenium(III)/ruthenium(II)-terpyridine chemistry have been performed. 2,2′:6′,2″-terpyridine as well as an anthracene-functionalized terpyridine were chosen as the graft ligands. Again, significant changes in the optical properties indicated successful complex formation. These results open new routes for the selective functionalization of beads by various polymers, biomaterials, and nano-objects, with the potential of leading to new types of heterogeneous catalysts.

*Acknowledgement:* This study was supported by the *Dutch Polymer Institute* (DPI), the *DFG*, and the *Fonds der Chemischen Industrie*. We would like to thank *Roy Reinierkens* for the AAS

measurements, *Nick Lousberg* for the SEM measurements, and *Richard Hoogenboom* for supplying the anthracene-functionalized terpyridine.

[1] [1a] B. Pugin, H.-U. Blaser, *Comprehensive Asymmetric Catalysis I-III* **1999**, *3*, 1367; [1b] A. Haynes, P. M. Maitlis, R. Quyoum, H. Adams, R. W. Strange, *Special Publication – Royal Society of Chemistry, Supported Catalysts and Their Applications* **2001**, *266*, 166.

[2] [2a] P. H. Seeberger, S. J. Danishefsky, *Acc. Chem. Res.* **1998**, *31*, 685; [2b] K. C. Nicolaou, R. Hanko, W. Hartwig, ''*Handbook of Combinatorial Chemistry*'', Wiley-VCH, Weinheim 2002; [2c] L. A. Thompson, J. A. Ellman, *Chem. Rev.* **1996**, *96*, 555; [2d] D. S. Thorpe, S. Walle, *Biochem. Biophys. Res. Commun.* **2000**, *269*, 591.

[3] [3a] T. S. Lee, D. W. Jeon, J. K. Kim, S. I. Hong, *Fibers Polym.* **2001**, *2*, 135; [3b] T. Godjevargova, A. Simeonova, A. Dimov, *J. Appl. Polym. Sci.* **2002**, *83*, 3036.

[4] C. U. Pittman, Jr., S. K. Wuu, S. E. Jacobson, *J. Catal.* **1976**, *44*, 87.

[5] [5a] E. C. Constable, *Adv. Inorg. Chem. Radiochem.* **1986**, *30*, 69; [5b] J.-M. Lehn, ''*Supramolecular Chemistry: Concepts and Perspectives*'', Wiley-VCH, Weinheim 1995; [5c] S. Bernhard, K. Takada, D. J. Diaz, H. D. Abruna, H. Murner, *J. Am. Chem. Soc.* **2001**, *123*, 10265.

[6] [6a] U. S. Schubert, O. Hien, C. Eschbaumer, *Macromol. Rapid Commun.* **2000**, *21*, 1156; [6b] U. S. Schubert, C. Eschbaumer, *Macromol. Symp.* **2001**, *163*, 177; [6c] B. G. G. Lohmeijer, U. S. Schubert, *Angew. Chem.* **2002**, *114*, 3980; *Angew. Chem. Int. Ed.* **2002**, *41*, 3825; [6d] J.-F. Gohy, B. G. G. Lohmeijer, U. S. Schubert, *Macromolecules* **2002**, *35*, 4560; [6e] U. S. Schubert, H. Hofmeier, *Macromol. Rapid Commun.* **2002**, *23*, 561; [6f] B. G. G. Lohmeijer, U. S. Schubert, *Angew. Chem.* **2002**, *114*, 3980; *Angew. Chem. Int. Ed.* **2002**, *41*, 3825.

[7] [7a] See, e.g.: R. J. Card, D. C. Neckers, *J. Am. Chem. Soc.* **1977**, *99*, 7733; [7b] R. J. Card, D. C. Neckers, *Inorg. Chem.* **1978**, *17*, 2345; [7c] R. J. Card, C. E. Liesner, D. C. Neckers, *J. Org. Chem.* **1979**, *44*, 1095; [7d] R. S. Drago, J. Gaul, A. Zombeck, D. K. Straub, *J. Am. Chem. Soc.* **1980**, *102*, 1033; [7e] R. S. Drago, E. D. Nyberg, A. G. El A'mma, *Inorg. Chem.* **1981**, *20*, 2461; [7f] P. Bosch, C. Campa, J. Camps, J. Font, P. De March, A. Virgili, *An. Quim., Ser. C: Quim. Org. Bioquim.* **1985**, *81*, 162; [7g] M. Antonietti, S. Lohmann, C. D. Eisenbach, U. S. Schubert, *Macromol. Rapid Commun.* **1995**, *16*, 283.

[8] T. Salditt, Q. An, A. Plech, C. Eschbaumer, U. S. Schubert, *Chem. Commun.* **1998**, 2731.

[9] R. Kröll, C. Eschbaumer, U. S. Schubert, M. R. Buchmeiser, K. Wurst, *Macromol. Chem. Phys.* **2001**, *202*, 645.

[10] K. Heinze, U. Winterhalter, T. Jannack, *Chem. Eur. J.* **2000**, *6*, 4203.

[11] D.-W. Yoo, S.-K. Yoo, C. Kim, J.-K. Lee, *J. Chem. Soc., Dalton Trans.* **2002**, 3931.

[12] W. E. Rapp, in: ''*Houben-Weyl*'', Vol. E22a, 4th edition, A. Felix, L. Moroder, C. Toniolo, Eds., Georg Thieme, Stuttgart 2002, p. 684.

[13] W. E. Rapp, *Comb. Chem.* **1997**, 65.

[14] E. C. Constable, M. D. Ward, *J. Chem. Soc., Dalton Trans.* **1990**, 1405.

[15] U. S. Schubert, S. Schmatloch, A. A. Precup, *Design. Monom. Polym.* **2002**, *5*, 211.

[16] U. S. Schubert, C. Eschbaumer, O. Hien, P. R. Andres, *Tetrahedron Lett.* **2001**, *42*, 4705.

[17] J. L. Bourdelande, C. Campa, J. Font, P. De March, *Eur. Polym. J.* **1989**, *25*, 197.

[18] H.-L. Kwong, W.-L. Wong, W.-S. Lee, L.-S. Cheng, W.-T. Wong, *Tetrahedron: Asymmetry* **2001**, *12*, 2683.

[19] H. Nishide, N. Shimidzu, E. Tsuchida, *J. Appl. Polym. Sci.* **1982**, *27*, 4161.

[20] [20a] B. P. Sullivan, J. M. Calvert, T. J. Meyer, *Inorg. Chem.* **1980**, *19*, 1404; [20b] T. Togano, N. Nagao, M. Tsuchida, H. Kumakura, K. Hisamatsu, F. S. Howell, M. Mukaida, *Inorg. Chim. Acta* **1992**, *195*, 221.

[21] B. G. G. Lohmeijer, U. S. Schubert, *Macromol. Chem. Phys.* **2003**, *204*, 1092.

 